Photoluminescence properties and exciton dynamics in monolayer WSe_2

Tengfei Yan, Xiaofen Qiao, Xiaona Liu, Pingheng Tan, and Xinhui Zhang[a)]
State Key Laboratory of Superlattices and Microstructures, Institute of Semiconductors, Chinese Academy of Sciences, P.O. Box 912, Beijing 100083, China

(Received 3 July 2014; accepted 24 August 2014; published online 9 September 2014)

In this work, comprehensive temperature and excitation power dependent photoluminescence and time-resolved photoluminescence studies are carried out on monolayer WSe_2 to reveal its properties of exciton emissions and related excitonic dynamics. Competitions between the localized and delocalized exciton emissions, as well as the exciton and trion emissions are observed, respectively. These competitions are suggested to be responsible for the abnormal temperature and excitation intensity dependent photoluminescence properties. The radiative lifetimes of both excitons and trions exhibit linear dependence on temperature within the temperature regime below 260 K, providing further evidence for two-dimensional nature of monolayer material. © *2014 AIP Publishing LLC*. [http://dx.doi.org/10.1063/1.4895471]

Monolayer tungsten diselenide (WSe_2) is a representative material of atomically thin transition metal dichalcogenides (TMDC), with high photoluminescence (PL) quantum yield[1] and large spin-orbit coupling induced spin splitting.[2,3] For TMDC family materials, exciton and trion binding energy are largely enhanced in strict 2D limit due to the reduced dimensionality and screening effect,[4–10] making it possible to observe exciton and trion related phenomena even at room temperature. The complicated excitonic features including neutral excitons, trions, localized excitons[7,10–12] as well as biexcitons[13] provide great opportunity to explore the rich excitonic physics in monolayer WSe_2 for both optoelectronics[14] and valleytronics applications.[15–20] Therefore, it is essentially important to explore and clarify the complex exciton properties as well as their emission dynamics. The recently reported emission helicity polarization is largely affected by the excitonic dynamics.[10,15,21] However, only limited transient optical studies on the exciton dynamics for TMDCs has been reported so far, and the results are not consistent with each other, showing striking material dependence.[10,21–27]

In this work, we report the steady-state PL and time resolved photoluminescence (TRPL) properties of monolayer WSe_2. The WSe_2 flakes are fabricated by mechanical exfoliation with adhesive tape from a bulk crystal (2D semiconductors, Inc.) onto SiO_2/Si substrates. The steady-state PL under the excitation of a 532 nm cw laser is collected by a microscope PL setup with Horiba Jobin Yvon iHR550 spectrometer. In the TRPL experiments, the sample was excited by 395 nm laser, which is the second harmonic generation output of a femtosecond Ti:sapphire laser (Tsunami, Spectra Physics). PL signal is collected using a Hamamatsu streak camera system with a time resolution of 20 ps. For the temperature dependent measurement, the sample was mounted in an Oxford helium-flow microscope cryostat (Microstat HiRes II).

Monolayer WSe_2 consists of one tungsten layer sandwiched by two selenium layers as illustrated in Fig. 1(a). The typical optical images of monolayer and bilayer WSe_2 are depicted in Fig. 1(b). The layer number of WSe_2 flakes are identified by their low-frequency shear (C) and layer breathing modes (LBM),[28] as well as room temperature PL signals, as shown in Figs. 1(c) and 1(d).[1,12,29] The band structure of monolayer WSe_2 is studied using $scGW_0$ method. The result is shown in the inset of Fig. 1(d), from which the direct bandgap at K point is determined to be 2.58 eV. Considering the exciton binding energy of 0.9 eV calculated by Ramasubramaniam,[6] the recombination energy of A exciton is estimated to be 1.68 eV. Though it is suggested that this exciton binding energy is overestimated,[30,31] all optical processes are surely modified in monolayer WSe_2 by excitonic effect. The numerically calculated A exciton emission energy is consistent with the PL experimental result of 1.63 eV here and existing reports[1,3,29]

The temperature dependent steady-state photoluminescence experiment is systematically carried out to investigate the excitonic properties of WSe_2. At temperatures below 120 K, two individual peaks are easily distinguished in

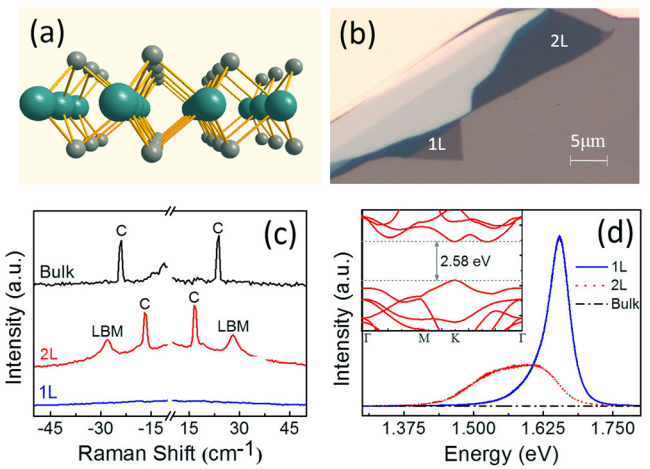

FIG. 1. (a) Schematic of monolayer WSe_2 structure; (b) Optical microscopic image of pre-marked WSe_2 monolayer, bilayer, and thin bulk flakes; (c) Raman spectra of monolayer, bilayer, and bulk WSe_2; (d) Room temperature PL spectrum of monolayer, bilayer, and bulk WSe_2, the inset shows the schematic of calculated band structure of monolayer WSe_2.

[a)]Electronic mail: xinhuiz@semi.ac.cn

monolayer sample PL response as shown in Fig. 2(a), with the details of typical PL response at 30 K and 100 K displayed in Fig. 2(b), respectively. The higher energy peak is labelled as FX. While the lower energy peak labelled as LX, with energy approximately 70 meV lower with respect to the FX peak at the temperature of 5 K and excitation power of 0.9 μW, is observed to dominate the low temperature PL response. Both the FX and LX PL peak centers exhibit abnormal temperature dependence.

To clarify the origin of both PL peaks, excitation power density dependent PL is investigated at 5 K and the main results are summarized in Fig. (3). To eliminate the possible signal fluctuation during PL detection, the presented PL spectra are normalized by the 520 cm^{-1} Raman peak of silicon substrate, which is linearly dependent on the excitation laser power. The integrated PL intensity I as a function of excitation power density L has been investigated for both emission peaks. It is seen that the relationship between PL intensity and excitation power follows the power law $I \propto L^k$, with k extracted to be 0.61 for the LX and 1.18 for FX emission, as presented by the solid fitting lines in Fig. 3(b). The LX PL peak gets saturated even at the lowest excitation fluence, suggesting the localized character of LX. The FX emission shows a nearly linear dependence, which is a character of direct recombination of excitons or trions. It is observed that the LX peak blueshifts as excitation intensity increases. Since increasing excitation intensity will cause band filling of the localized energy states, giving rise to the blueshifts of LX emission. Possible heating effect caused by increasing laser power is excluded, as no apparent broadening of PL spectra or shift of E_{2g} Raman mode[12] are observed when varying the excitation power. Meanwhile, by referring to the Raman spectra of the sample, the peak of E_{2g} mode does not exhibit any shift when increasing excitation power.

The localized excitons with typical PL emission centered between 1.64 and 1.70 eV at low temperature in monolayer WSe_2 have been observed.[7,10,11] Here, the LX emission peak characterizes an asymmetric line shape with a sharp high-energy cutoff and an exponential low-energy tail, and is

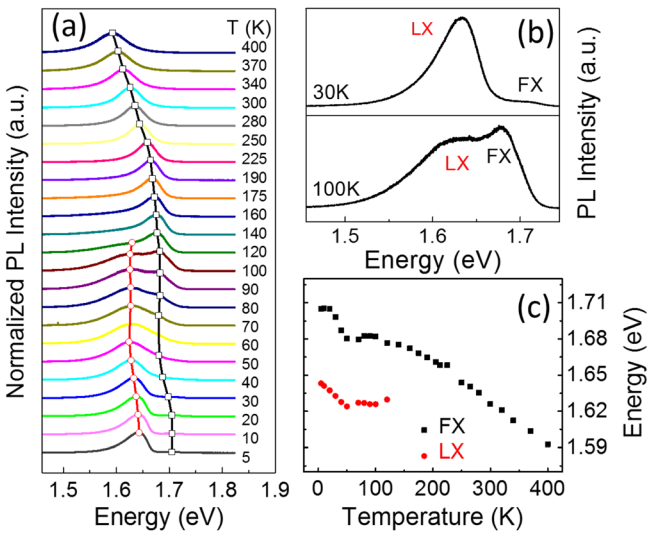

FIG. 2. (a) Normalized PL spectra of WSe_2 at different temperature; (b) PL spectrum taken at 30 K and 100 K, respectively; (c) Free exciton (black) and localized exciton (red) emission energy at different temperature.

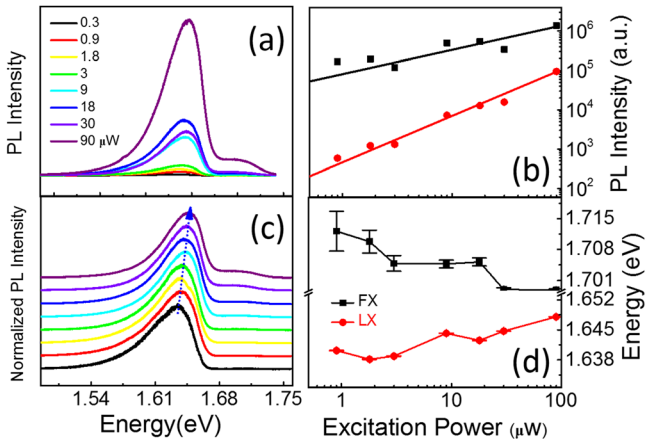

FIG. 3. (a) PL intensity at different excitation power normalized by Si 520 cm^{-1} Raman peak; (b) The integrated PL intensity at different excitation power; (c) Normalized PL response of WSe_2 at different excitation power; (d) Excitation power dependent PL peak energies of FX (black) and LX (red) peak positions. All data presented here are measured at 5 K.

thermally quenched with increasing temperature and becomes unnoticeable at temperatures above 120 K, shown in Fig. 2(a). These features observed for LX peak are usually considered as the evidence of disorder-related effects, which have been previously demonstrated in GaNAs/GaAs and InGaN/GaN quantum wells (QWs).[32,33] SiO_2/Si substrates usually display a large surface roughness of 4–8 Å, complex exciton features associated with surface roughness as well as the residual contaminants at the WSe_2/SiO_2 interface or residues deposited after the exfoliation step will be expected.[12] As the random fluctuations of crystallographic defect distribution or interface inhomogeneity may smear the band edge and form tail in the density of states extending into the bandgap, photo-excited excitons can be trapped by the localized states at the band tails at low temperatures, leading to the observed asymmetric lineshape of the PL spectra. The low-energy tail of the PL response reflects the energy distribution of the density of states within the band tails, while the high-energy side cutoff corresponds to the mobility edge.[32]

The localized-state related PL emission shows characteristic thermal behaviour, as shown in Figs. 2(a) and 2(c). When temperature increases, trapped excitons can be thermally activated into the delocalized states and captured by the competing nonradiative decay channels or recombine as free excitons. Therefore, it is expected that the intensity of localized exciton emission decreases monotonically with increasing temperature while free exciton emission increases, which is exactly what we observed for the ones labelled as LX and FX, respectively. The shallowly localized carriers are first thermally activated to the delocalized states, so the peak position exhibits redshift when temperature increases at low temperature regime below 50 K. With further increase of temperature, LX peak shows blueshifts as carriers in band-tails redistribute.[33]

The low temperature FX PL response measured here exhibits broader linewidth and redshift of about 45 meV with respect to the reported A exciton recombination at corresponding temeperature,[7,10,11] though the room temperature PL response agrees well with previous reports. Based on the temperature and excitation power density dependent studies,

we argue that the redshifted FX peak at low temperature regime are not separated spectrally due to broad transitions as usually observed in MoS_2. While with increasing temperature, the exciton recombination emission dominates the PL response as trions tend to ionize at temperatures close to 300 K, considering the trion binding energy of 25–30 meV.[7,10] Trion associated emission may exist in our case because of the existence of excess background carriers resulting from the unintentional doping of the studied WSe_2 bulk crystal, in addition to the photo-excited carriers, and the photo-ionized carriers trapped on the dopants.[8] Free exciton and trion emissions are merged together spectrally, giving rise to overall emission redshift and broader linewidth. This may result from the surface roughness and contamination during exfoliation process, and hereby the increased carrier-carrier and carrier-defect scatterings, evidenced by the dominant localized-exciton-emission at low temperature. The estimated Stokes shift of 5 meV at room temperature, obtained by comparing the PL and absorption spectra, suggests the existence of background carriers, since the Stokes shift is proportional to the Fermi energy,[9] but whether the excess carriers are electrons or holes is unclear yet.

It is seen that FX emission exhibits redshifts when temperature increases from 5 K to 50 K, since defects would ionize more efficiently at higher temperatures, lifting the Fermi level and providing more excess free carriers favouring trion formation. Meanwhile, the trion emission energy is reduced as the energy split between the trion and exciton emission equals to the energy required to dissociate a hole from a trion and obeys $\hbar\omega_{X^0} - \hbar\omega_{X^+} = E_{X^+} + E_F$.[9,34] Here, ω_{X^0} and ω_{X^+} are the frequencies of free excitons and trions emission, respectively; E_{X^+} is the trion emission energy and E_F is the Fermi energy. With rising temperature higher than 50 K, trions ionize so that the exciton emission starts to dominate the PL response, and the PL envelope exhibits a slight blueshift. With furthermore increase of temperature, the exciton emission peak redshifts due to bandgap reduction. The excitation intensity dependent emission energy shifts measured at 5 K, as displayed in Fig. 3(d), can be understood well by following the same discussions as above. The FX peak exhibits redshifts with increasing excitation density since the Fermi level is lifted as the results of the increased amount of photo-ionized dopants.

A series of temperature dependent transient PL spectra are shown in Fig. 4(a), obtained by spectrally averaging each TRPL data in a 4 nm-wide region centered at the FX peak of monolayer WSe_2. Two individual components can be deduced from results of the TRPL response that can be well fitted with a biexponential decay function. Temperature dependence of the two distinct decay time constants extracted is shown in Fig. 4(b). Both time constants increase with rising temperature and drop with further increase of temperature above 260 K. The short-lived component varies from 20 ps at 130 K to 60 ps at 260 K, while the long-lived component varies from 70 ps at 130 K to 250 ps at 260 K.

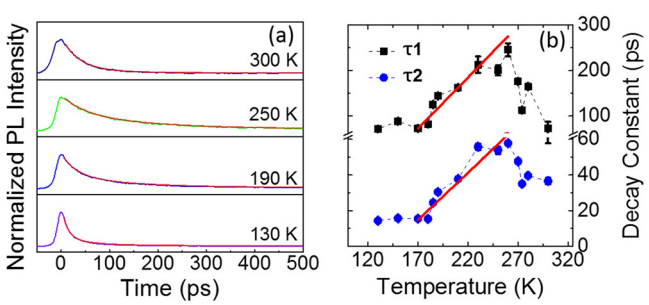

FIG. 4. (a) Normalized TRPL of WSe_2 at different temperatures with biexponential fit shown in red solid lines; (b) The extracted two time constants at different temperatures (the red line is linear fit).

As discussed previously, trions could exist even at room temperature considering the large trion binding energy. Low temperature steady-state PL spectra show that trion and exciton emission spectrally overlap each other for our investigated sample. The two decay processes observed via TRPL measurement therefore correspond to the trion and exciton radiative decay time distinctively. Nonradiative recombination can be safely neglected at temperatures between 120 K and 220 K, since the integrated PL intensity of FX peak is almost constant in steady-state PL measurement. The long-lived component is thus attributed to the exciton radiative decay time, while the short-lived component in tens of picosecond is tentatively assigned to associate with the trion radiative decay time, since a few times shorter radiative lifetime of trions comparing to the excitons is often observed in GaAs QWs.[35,36] The assignment of both trion and exciton associated radiative decay time is furthermore supported by their temperature dependent behavior within the temperature regime below 260 K, as presented in Fig. 4. It is observed that both components show approximately linear dependence on temperature, and follow the same temperature dependent behavior as that for two dimensional semiconductor structures,[35,37] which obeys: $\tau_x^{2D} \propto E_B^{-1} M\Delta(T)/\mu r(T)$. Here, τ_x^{2D} is the lifetime of excitons; E_B is exciton binding energy; $M = m_e^* + m_h^*$ is the sum of electron and hole effective mass and μ is the reduced mass of exciton. $\Delta(T)$ is the linewidth of exciton luminescence and r(T) is the possibility of exciton states located in the energy range of $\Delta(T)$, which describes the ratio of states contributing to the radiative recombination for all states using Maxwell-Boltzmann statistics. In the temperature regime of 170–260 K, both components are found to follow the relation of $\tau \propto kT$, as indicated by the red fitting lines in Fig. 4(b). The linear dependence on temperature for both decay constants implies that both trions and excitons are delocalized above 170 K and show free character. However, their decay process is insensitive to temperature below 170 K, which may be related to the weak localization due to surface roughness or crystallographic imperfection. The similar constant radiative decay time due to localization at very low temperature was also observed and interpreted previously in GaAs- and CdTe-based QWs.[35,37–39] At temperatures higher than 260 K, the nonradiative recombination such as exciton-acoustic phonon scattering is enhanced and $\Delta(T)$ is comparable to r(T). So the decay time τ drops above 260 K.

Recent TRPL study for MoS_2 by Lagarde *et al.* suggested that the short-lived decay component reported by Korn *et al.*[22] and Huang *et al.*[23] may be related to the intrinsic exciton lifetime rather than limited by the nonradiative recombination.[21] The linear dependence of both decay constants on temperature revealed in our case suggests that the

decay components are related to the direct radiative recombination process in WSe_2.

In summary, we have studied the exciton/trion emission and related dynamics of unintentionally doped monolayer WSe_2 with temperature dependent PL and TRPL spectroscopy. Both localized and delocalized exciton emissions have been observed and confirmed. The competition between trion and exciton emissions results in an S-shaped PL peak energy-temperature dependence. Temperature dependent TRPL measurements provide further evidence for 2D nature of monolayer material and the lifetimes of both excitons and trions are determined as well. Our studies provide evidence for the localized-exciton related light emission and reveal the complex photoluminescence properties of monolayer WSe_2, which are essentially important to achieve TMDCs-based novel optoelectronics and valleytronics.

This work was supported by the National Basic Research Program of China (No. 2011CB922200) and the National Natural Science Foundation of China (Nos. 11274302 and 11474276).

[1]W. Zhao, Z. Ghorannevis, L. Chu, M. Toh, C. Kloc, P.-H. Tan, and G. Eda, ACS Nano **7**, 791 (2012).
[2]Z. Zhu, Y. Cheng, and U. Schwingenschlögl, Phys. Rev. B **84**, 153402 (2011).
[3]H. Zeng, G.-B. Liu, J. Dai, Y. Yan, B. Zhu, R. He, L. Xie, S. Xu, X. Chen, W. Yao *et al.*, Sci. Rep. **3**, 1608 (2013).
[4]J. S. Ross, S. Wu, H. Yu, N. J. Ghimire, A. M. Jones, G. Aivazian, J. Yan, D. G. Mandrus, D. Xiao, W. Yao *et al.*, Nat. Commun. **4**, 1474 (2013).
[5]B. Stebe and A. Ainane, Superlattices Microstruct. **5**, 545 (1989).
[6]A. Ramasubramaniam, Phys. Rev. B **86**, 115409 (2012).
[7]A. M. Jones, H. Yu, N. J. Ghimire, S. Wu, G. Aivazian, J. S. Ross, B. Zhao, J. Yan, D. G. Mandrus, D. Xiao *et al.*, Nat. Nanotechnol. **8**, 634 (2013).
[8]A. Mitioglu, P. Plochocka, J. Jadczak, W. Escoffier, G. Rikken, L. Kulyuk, and D. Maude, Phys. Rev. B **88**, 245403 (2013).
[9]K. F. Mak, K. He, C. Lee, G. H. Lee, J. Hone, T. F. Heinz, and J. Shan, Nat. Mater. **12**, 207 (2013).
[10]G. Wang, L. Bouet, D. Lagarde, M. Vidal, A. Balocchi, T. Amand, X. Marie, and B. Urbaszek, Phys. Rev. B **90**, 075413 (2014).
[11]S. Tongay, J. Suh, C. Ataca, W. Fan, A. Luce, J. S. Kang, J. Liu, C. Ko, R. Raghunathanan, J. Zhou *et al.*, Sci. Rep. **3**, 2657 (2013).
[12]H. Sahin, S. Tongay, S. Horzum, W. Fan, J. Zhou, J. Li, J. Wu, and F. Peeters, Phys. Rev. B **87**, 165409 (2013).
[13]A. Thilagam, J. Appl. Phys. **116**, 053523 (2014).
[14]J. S. Ross, P. Klement, A. M. Jones, N. J. Ghimire, J. Yan, D. G. Mandrus, T. Taniguchi, K. Watanabe, K. Kitamura, W. Yao, D. H. Cobden, and X. Xu, Nat. Nanotechnol. **9**, 268 (2014).
[15]K. F. Mak, K. He, J. Shan, and T. F. Heinz, Nat. Nanotechnol. **7**, 494 (2012).
[16]D. Xiao, G.-B. Liu, W. Feng, X. Xu, and W. Yao, Phys. Rev. Lett. **108**, 196802 (2012).
[17]H. Zeng, J. Dai, W. Yao, D. Xiao, and X. Cui, Nat. Nanotechnol. **7**, 490 (2012).
[18]D. Xiao, W. Yao, and Q. Niu, Phys. Rev. Lett. **99**, 236809 (2007).
[19]W. Yao, D. Xiao, and Q. Niu, Phys. Rev. B **77**, 235406 (2008).
[20]T. Cao, G. Wang, W. Han, H. Ye, C. Zhu, J. Shi, Q. Niu, P. Tan, E. Wang, B. Liu *et al.*, Nat. Commun. **3**, 887 (2012).
[21]D. Lagarde, L. Bouet, X. Marie, C. Zhu, B. Liu, T. Amand, P. Tan, and B. Urbaszek, Phys. Rev. Lett. **112**, 047401 (2014).
[22]T. Korn, S. Heydrich, M. Hirmer, J. Schmutzler, and C. Schüller, Appl. Phys. Lett. **99**, 102109 (2011).
[23]H. Shi, R. Yan, S. Bertolazzi, J. Brivio, B. Gao, A. Kis, D. Jena, H. G. Xing, and L. Huang, ACS Nano **7**, 1072 (2014).
[24]R. Wang, B. A. Ruzicka, N. Kumar, M. Z. Bellus, H.-Y. Chiu, and H. Zhao, Phys. Rev. B **86**, 045406 (2012).
[25]C. Mai, A. Barrette, Y. Yu, Y. Semenov, K. W. Kim, L. Cao, and K. Gundogdu, Nano Lett. **14**, 202 (2013).
[26]S. Sim, J. Park, J.-G. Song, C. In, Y.-S. Lee, H. Kim, and H. Choi, Phys. Rev. B **88**, 075434 (2013).
[27]Q. Wang, S. Ge, X. Li, J. Qiu, Y. Ji, J. Feng, and D. Sun, ACS Nano **7**, 11087 (2013).
[28]X. Zhang, W. P. Han, J. B. Wu, S. Milana, Y. Lu, Q. Q. Li, A. C. Ferrari, and P. H. Tan, Phys. Rev. B **87**, 115413 (2013).
[29]P. Tonndorf, R. Schmidt, P. Böttger, X. Zhang, J. Börner, A. Liebig, M. Albrecht, C. Kloc, O. Gordan, D. R. Zahn *et al.*, Opt. Express **21**, 4908 (2013).
[30]D. Y. Qiu, H. Felipe, and S. G. Louie, Phys. Rev. Lett. **111**, 216805 (2013).
[31]C. Zhang, A. Johnson, C.-L. Hsu, L.-J. Li, and C.-K. Shih, Nano Lett. **14**, 2443 (2014).
[32]I. Buyanova, W. Chen, G. Pozina, J. Bergman, B. Monemar, H. Xin, and C. Tu, Appl. Phys. Lett. **75**, 501 (1999).
[33]Y.-H. Cho, G. Gainer, A. Fischer, J. Song, S. Keller, U. Mishra, and S. DenBaars, Appl. Phys. Lett. **73**, 1370 (1998).
[34]V. Huard, R. Cox, K. Saminadayar, A. Arnoult, and S. Tatarenko, Phys. Rev. Lett. **84**, 187 (2000).
[35]D. Sanvitto, R. Hogg, A. Shields, D. Whittaker, M. Simmons, D. Ritchie, and M. Pepper, Phys. Rev. B **62**, R13294 (2000).
[36]G. Finkelstein, V. Umansky, I. Bar-Joseph, V. Ciulin, S. Haacke, J.-D. Ganiere, and B. Deveaud, Phys. Rev. B **58**, 12637 (1998).
[37]J. Feldmann, G. Peter, E. Göbel, P. Dawson, K. Moore, C. Foxon, and R. Elliott, Phys. Rev. Lett. **60**, 243 (1988).
[38]V. Ciulin, P. Kossacki, S. Haacke, J.-D. Ganiere, B. Deveaud, A. Esser, and T. Wojtowicz, Phys. Rev. B **62**, R16310 (2000).
[39]D. Citrin, Phys. Rev. B **47**, 3832 (1993).